Joint Optimization of Signal Waveforms and Filters for Long-Range MIMO Radars

PAVEL BEZOUŠEK AND SIMEON KARAMAZOV[ID]

Faculty of Electrical Engineering and Informatics, University of Pardubice, 532 10 Pardubice, Czech Republic

Corresponding author: Simeon Karamazov (simeon.karamazov@upce.cz)

ABSTRACT This paper describes a new cyclic algorithm for minimization of signal sidelobes and crosstalk in multiple-input multiple-output (MIMO) radar. The designed algorithm, called SWAP by the authors, is suitable mainly for long-range radars, such as ground-based surveillance, approach, or weather radar. The minimization of energy or amplitude of side lobes, and crosstalk were used as the optimization criteria. The effect of the Doppler shift is also included in the optimization. Although the optimized signals do not maintain a strictly constant envelope, the peak-to-average power ratio (PAR) can be maintained below 1.7. This value is acceptable, especially for radars with modern transmitters based on GaN HEMTs. The algorithm allows for any arbitrary choice of elements weights, enabling the optimization of calculations for a wide range of applications. This paper also presents the results of algorithm testing under various conditions. The designed algorithm makes it possible to suppress the side lobes and crosstalk by up to 20 dB more than the matched filters. These results were achieved at the cost of a slight deterioration in signal-to-noise ratio (SNR) loss (less than 1 dB) and an increase in PAR (up to 2). The resolution of weak close targets is also slightly deteriorated. The algorithm converged quickly, and already after ten or 20 iterations, the results changed only minimally.

INDEX TERMS Crosstalk, Doppler effect, iterative optimization, matched filter, MIMO radar, peak to average power ratio, quadratic programming, side lobe, signal to noise ratio.

I. INTRODUCTION

MIMO radars, with a number of transmitted signals and receivers, provide additional degrees of freedom in the design of modern systems with adaptable properties, particularly in area coverage. For example, using M transmitters and R receivers, up to (M × R) independent measurements from a single object can be used for processing. This is used to enhance the detection quality, increase the accuracy of its location, speed up the information update, and improve interesting object recognition (e.g., the suppression of unconscious reflections and other interference). Two types of MIMO radar systems are typically distinguished: distributed and collocated systems. The distance between the antennas of collocated systems is usually of the order of only a few wavelengths, whereas in distributed systems, the distances between the antennas are much greater than the system space resolution. In this study, we deal with signals and filters designed mainly for systems with collocated antennas. However, some results can be used even for distributed systems.

Recently, considerable attention has been paid to the optimization of signal modulation and compression (separation)

The associate editor coordinating the review of this manuscript and approving it for publication was Chengpeng Hao[ID].

filters for MIMO radars. A large number of these publications, as demonstrated in [1]–[9], deal with the signals of a constant envelope and matched filters that automatically guarantee the maximum compression gain, that is, the minimum SNR loss. The constant envelope constraint allows us to optimize transmitter efficiency by utilizing the maximum available transmitter power. Under these conditions, only the phases of the transmitted signals were optimized. Computationally efficient sophisticated algorithms have been developed for signal design, optimizing the minimum integrated side lobe level (ISL) criterion under various constraints as shown in [4] and [7]–[9]. (Here, also crosstalk is assumed under the term ''side lobes''.) The ISL criterion is beneficial mainly for relatively homogeneous clutter such as rain, fog, or a calm sea surface. In the case of clutter with high reflection dynamics, such as in an urban area or heavily undulating terrain, signals showing a minimum peak side lobe (PSL) are better suited. Therefore, in addition to the minimum ISL criterion, this study addresses also PSL minimization.

In addition, the a priori choice of matched filters and strict requirements of a constant signal envelope significantly limit the side lobe and crosstalk suppression. However, many authors have shown that significantly better side-lobe suppression (up to hundreds of dB) can be achieved by

selecting only a limited range of side lobes for optimization, for example, by using WeCAN, AISO, IAG and related algorithms, as demonstrated in [5] and [10]–[15]. The remaining (i.e., not-selected) side lobes show only a poor suppression. Such signals are particularly useful for long-pulse and CW radars. Furthermore in these systems the penetration of the transmitted signals into the receiver frequently limits the maximum radar range and a perfect side-lobe suppression, even at bounded time lags, can help overcome this limitation.

On the other hand, in long range radars with short pulses a good suppression of all sidelobes and crosstalk is necessary. From the practice of SISO and SIMO radars it is known, that using mismatched filters, can significantly improve side lobe suppression according to [16]–[18]. Thus the procedure of mismatched filter design, which can be solved directly, became the basis of the simultaneous optimization of the signals and filters presented in this article. Using the commutative property of convolution, an algorithm is created that alternately optimize coefficients of the separation filters and samples of the complex envelopes of the transmitted signals. However, this procedure cannot ensure neither zero SNR loss nor a strictly constant signal amplitude.

The requirement of a constant envelope of the transmitted signals is important for the transmitter efficiency and maximum utilization of the available power. These qualities are closely related to the PAR of a transmitted signal. To avoid nonlinear distortion of the transmitted signal, which leads to degradation of the radar resolution and signal side lobes, it is appropriate to set the mean transmitted power significantly below P_{sat}/PAR, where P_{sat} is the saturated transmitter power. The excellent linearity of modern power amplifiers based on GaN transistors and new results in digital predistortion linearizers [19]–[25] make it possible to approach or even exceed the P_{sat}/PAR value. This allowed us to loosen the strict constant signal envelope requirements, which facilitated further suppression of the sidelobes and crosstalk by up to 20 dB.

In this study, we addressed the optimization of filters and signals for ground-based long-range MIMO radars. For these radars, the pulse length is typically significantly shorter than the longest return time of the reflected signals. Therefore, it is important that the time-side lobes are sufficiently suppressed at all lags from the main lobe. Furthermore, ground clutter frequently consists of reflections from isolated objects with a high RCS (Radar Cross Section) that significantly exceeds the RCS of the desired targets. Therefore, in addition to the minimum ISL criterion, the minimum PSL criterion is applied. However, a reduction in the compression efficiency of the filters by $0.5 - 1$ dB, or a partial deterioration of the resolution of weak close targets is not critical in such an environment. Eventually, in a better clutter situation, a matched filter with a narrower peak but higher sidelobes can be used. An important feature of these radars is the use of the Doppler effect to distinguish targets moving at different speeds. Therefore, the requirements for high-quality processing of Doppler-shifted signals in a sufficient frequency range were also included.

Radars of this type use MIMO technology mainly to speed up radar information updates over large areas. Multiple transmitted signals allow the radar to simultaneously perform multiple tasks. Therefore, the number of transmitted signals is not large, and usually range only from two to ten. The individual signals are narrowband, and their bandwidths are generally significantly smaller than the bandwidths available for these services. Thus, it is possible to use frequency diversification for signal separation, which further facilitates crosstalk suppression.

For this purpose, a simple cyclic approximation algorithm was developed, which enabled to design transmitted signal modulation and separation/compression filters achieving significantly better suppression of the side lobes and crosstalk at the expense of a slight relaxation in the SNR loss and PAR. Both the ISL and PSL minimization criteria were used with constraints on the signal power, filter gain, PAR, and SNR loss.

The organization of this article is as follows:

In Section 2, the system under consideration is briefly described and the quantities and basic relations used in this study are presented. The minimization criteria and ISL and PSL metrics are also introduced. Proceeding from well-known basic expressions, we integrate the Doppler effect and sample weights in these metrics and transform the relations to the form, which is convenient for deriving the optimization algorithm. In Section 3, a new cyclic algorithm, SWAP, is introduced along with the expressions of the relevant metrics that are suitable for the execution of this algorithm. Section 4 presents the results of testing the algorithm under selected conditions.

II. MATHEMATICAL DESCRIPTION
A. PROBLEM FORMULATION
We consider a MIMO radar using M transmitted signals $s_m(i) = x_m(i) \exp(j\omega_0 t)$, where ω_0 is the carrier frequency. Each antenna emits pulses of length $\tau = N.T_S$, where N is the number of samples of the signal complex envelope $\{x_m(i)\}_{i=1, m=1}^{N, M}$, and T_S is the sampling period. The complex envelopes of the frequency-diversified signals are given by the expression $x_m(i) = \exp[j\Phi(i) + j2\pi f_m i T_s]$. Phase $\Phi(i)$ represents LFM or NLFM modulation, f_m is the central frequency (subcarrier) of the complex envelope of the mth signal $f_m = [m - 1 - (M - 1)/2]\kappa B$, where $\kappa > 1$ is a dimensionless parameter that determines the distance between adjacent subcarriers, and B is the bandwidth of each signal.

Compression and separation filters $\{q_\mu(k)\}_{k=1, \mu=1}^{K, M}$ compress pulses, and separate signals of individual transmitters (where K is the filter order). To facilitate the comparison of the following results, we chose the number of signal samples N to be equal to the number of uncorrelated noise samples in the pulse length interval τ: $N = BW.\tau$, where BW is the bandwidth of the entire set of signals. From the samples of complex envelopes of the received signals $x_m(i)$ and the filter coefficients $q_\mu(k)$ we create column vectors $\mathbf{x}_m$

and $\mathbf{q}_\mu$, such that

$$\mathbf{x}_m = \left[x_m(1), \ldots, x_m(i), \ldots, x_m(N) \right]^T,$$
$$m = 1, 2, \ldots, M, \quad (1)$$
$$\mathbf{q}_\mu = \left[q_\mu(1), \ldots, q_\mu(k), \ldots, q_\mu(K) \right]^T,$$
$$\mu = 1, 2, \ldots, M. \quad (2)$$

The signals at the filter outputs are linear combinations of convolutions

$$\mathbf{z}_{m\mu} = \mathbf{x}_m * \mathbf{q}_\mu = \begin{bmatrix} z_{m\mu}(1-K) \\ \vdots \\ z_{m\mu}(N-1) \end{bmatrix},$$

$$z_{m\mu}(n) = \sum_{k=1}^{n+K} x(n+K+1-k) . q(k), \quad (3)$$

where $n = 1-K, \ldots, 0, \ldots, N-1$; if $n > N$, the signal samples are $x_m(n) = 0$.

If matched filters are used, the convolutions $\mathbf{z}_{m\mu}$ are equal to the corresponding cross-correlation functions. For an easier comparison with matched filters, we chose the filter order K to be equal to the number of signal samples in our further calculations. That means $K = N$.

If we create a Toeplitz matrix $\boldsymbol{\Lambda}$ from complex envelope vectors $\mathbf{x}_m$ and a matrix $\mathbf{Q}$ from the filter vectors $\mathbf{q}_\mu$. Then, all convolutions in (3) can be rewritten in matrix form as follows:

$$\mathbf{Z} = \begin{bmatrix} \mathbf{z}_{11} & \cdots & \mathbf{z}_{1M} \\ \vdots & & \vdots \\ \vdots & & \vdots \\ \mathbf{z}_{M1} & \cdots & \mathbf{z}_{MM} \end{bmatrix} = \boldsymbol{\Lambda}.\mathbf{Q}$$

$$= \boldsymbol{\Lambda}. \begin{bmatrix} q_1(1) & \cdots & q_M(1) \\ \vdots & & \vdots \\ \vdots & & \vdots \\ q_1(K) & \cdots & q_M(K) \end{bmatrix}, \quad (4)$$

where

$$\boldsymbol{\Lambda} = \begin{bmatrix} \boldsymbol{\Lambda}_1 \\ \boldsymbol{\Lambda}_2 \\ \vdots \\ \vdots \\ \boldsymbol{\Lambda}_M \end{bmatrix},$$

$$\boldsymbol{\Lambda}_m = \begin{bmatrix} x_m(1) & 0 & \cdots & 0 \\ x_m(2) & x_m(1) & \ddots & \vdots \\ \vdots & x_m(2) & \ddots & 0 \\ x_m(N) & \vdots & \ddots & x_m(1) \\ 0 & x_m(N) & \ddots & x_m(2) \\ \vdots & \ddots & \ddots & \vdots \\ 0 & \cdots & 0 & x_m(N) \end{bmatrix} \quad (5)$$

B. BASIC OPTIMIZATION CRITERIA

The aim is to design signals and filters, that is, elements of vectors $\mathbf{x}_m$ and $\mathbf{q}_\mu$ so, that the mixture of all received signals is divided by filters into channels according to individual transmitters, and simultaneously, the pulses are compressed into the main lobe. This means that all elements of the convolution matrix, $\mathbf{Z}$, for which $m \neq \mu$, must be as small as possible because there is crosstalk between individual signals. The same is true for the elements of the side lobes, that is, for convolutions with $m = \mu$ and $n \neq 0$.

To prepare a simultaneous optimization procedure for filters and signals, we start with the well-known simple relations for the ISL and PSL metrics, assuming neither sample weights nor Doppler effect. We then rearrange these expressions to better suit the optimization of the filters. In the next paragraph, the Doppler effect and weights are added to both the metrics.

1) MINIMUM ISL CRITERION

Suppression of energy in the signal side lobes and crosstalk at the outputs of the compression filters are ensured by minimizing the expression

$$\text{ISL} = \sum_{n=1-N, n\neq 0}^{N-1} \left[\sum_{m=1}^{M} |z_{mm}(n)|^2 \right]$$
$$+ \sum_{n=-N+1}^{N-1} \sum_{\mu=1}^{M} \sum_{m=1, m\neq\mu}^{M} |z_{m\mu}(n)|^2, \quad (6)$$

subjected to normalization conditions $\mathbf{x}_m^T \cdot \mathbf{q}_m \equiv z_{mm}(0) = C$, where C is a chosen positive constant. Using matrices $\boldsymbol{\Lambda}$ and $\mathbf{Q}$ defined above, we can easily convert (6) into a more compact form:

$$\text{ISL} = \| \boldsymbol{\Lambda}.\mathbf{Q} - C\mathbf{J} \|^2, \quad (7)$$

where $\|.\|$ is the Frobenius norm and

$$\mathbf{J} = \begin{bmatrix} \mathbf{j}_{11} & \cdots & \mathbf{j}_{M1} \\ \vdots & & \vdots \\ \vdots & & \vdots \\ \mathbf{j}_{M1} & \cdots & \mathbf{j}_{MM} \end{bmatrix}, \quad \mathbf{j}_\mu = \begin{bmatrix} \mathbf{j}_{1\mu} \\ \vdots \\ \vdots \\ \mathbf{j}_{M\mu} \end{bmatrix},$$

$$\mathbf{j}_{m\mu} = \begin{bmatrix} 0 \\ \vdots \\ \delta_{m\mu} \\ \vdots \\ 0 \end{bmatrix}, \quad \delta_{mm} = 1, \ \delta_{m\mu} = 0 \text{ for } m \neq \mu. \quad (8)$$

If we apply ISL minimization only to the filter coefficients, it is better to use another equivalent form of metric (7).

$$\text{ISL} = \sum_{\mu=1}^{M} \| \boldsymbol{\Lambda} \cdot \mathbf{q}_\mu - C\mathbf{j}_\mu \|^2. \quad (9)$$

As the matrix $\boldsymbol{\Lambda}$ does not depend on the filter coefficients, but only on the signal samples, minimization can be performed

for each $\mathbf{q}_\mu$ independently. The problem can then be solved analytically [26], and the optimized coefficients of the individual filters can be expressed as follows:

$$\mathbf{q}_\mu = \arg\left\{\min_{\mathbf{q}_\mu} \left\| \mathbf{\Lambda}.\mathbf{q}_\mu - C\mathbf{j}_\mu \right\|^2\right\} \qquad (10)$$

2) MINIMUM PSL CRITERION

This criterion requires that the maximum amplitudes of the side lobes and crosstalk be minimized. Considering the normalization condition $\mathbf{x}_m^T \cdot \mathbf{q}_m \equiv z_{mm}(0) = C$, the metric PSL for this criterion can be written in the form:

$$\text{PSL} = \max\left\{ \max_{m,n\neq0}\{|z_{mm}(n)|\}, \max_{n,m,\mu\neq m} |z_{m\mu}(n)| \right\}$$
$$= \|\mathbf{\Lambda}.\mathbf{Q} - C\mathbf{J}\|_\infty, \qquad (11)$$

where $\|.\|_\infty$ is the maximum matrix norm.

Again, the PSL can be written in a modified form, which is advantageous for the subsequent procedure.

$$\text{PSL} = \|\mathbf{\Lambda}.\mathbf{Q} - C\mathbf{J}\|_\infty$$
$$= \max_\mu \|\mathbf{\Lambda}.\mathbf{q}_\mu - C\mathbf{j}_\mu\|_\infty. \qquad (12)$$

If only the optimization of filter coefficients is assumed, the minimization breaks down to the minimization of metrics $\|\mathbf{\Lambda}.\mathbf{q}_\mu - C\mathbf{j}_\mu\|_\infty$ for individual filters separately, which can be solved by convex programming methods quadratically constrained quadrature programming (QCQP), as was demonstrated in [26] and [27].

$$\mathbf{q}_\mu = \arg\left\{\min_{\mathbf{q}_\mu} \left\| \mathbf{\Lambda}.\mathbf{q}_\mu - C\mathbf{j}_\mu \right\|_\infty\right\}. \qquad (13)$$

As already mentioned, for long-range radars, where the return time of the signal T_D is much longer than the transmitted pulse length τ, $T_D \gg \tau$, linear, and nonlinear frequency-modulated signals (LFM and NLFM) are often used, mainly because these modulations tolerate the Doppler frequency shift of the received signals well. Through the frequency diversification of such signals, a set of FD LFM and FD NLFM signals can be created for these types of radars. (In our demonstrations, we used nonlinear frequency modulation with a Taylor-shaped spectrum). Even with the application of matched filters, the suppression of side lobes and crosstalk of these signals, [10], [15], are significantly better than those calculated using the CAN algorithm or similar methods.

Fig. 1 shows the output waveforms of the mismatched compression and separation filters in the system with $M = 4$ transmitted signals, calculated according to the ISL and PSL criteria, applied only to the filter coefficients. The subfigures in each row show responses of one filter to the four transmitted signals. In the columns the signal outputs of the individual filters fed by the same transmitted signal are displayed.

For comparison, the output from the matched filters was also provided. It can be seen, that by abandoning the requirement of matched filters, the side lobes and crosstalk at the filter outputs can be further suppressed by about 10 dB.

C. INCLUSION OF THE DOPPLER EFFECT AND WEIGHTING

The previous procedure made it possible to determine the elements of the compression filters such that the filter outputs were improved compared with the matched filters (Fig. 1). However, it was not possible to include signals affected by the Doppler shift during optimization. In multiple publications, the Doppler effect is integrated into optimization simply by adding the signal responses affected by the Doppler shift to the minimized metrics (e.g., [13]–[15]), and we use the same method. To derive the SWAP algorithm procedure, we introduce the following notation.

The Doppler effect changes the signal complex envelope samples to $x_m^{(l)}(i) = x_m(i)\exp[j(i-1)\omega_{Dl}t_s]$, containing a Doppler frequency shift, ω_{Dl}.

The product $\omega_{Dl}t_s = \omega_{Dl}/BW$ is the phase increment between the adjacent samples of the signal with the lth Doppler frequency shift. In the matrix form, the Doppler shift can be expressed by modifying the signal vector (1)

$$\mathbf{x}_m^{(l)} = \mathbf{E}_l \cdot \mathbf{x}_m = \left[x_m^{(l)}(1)\ldots x_m^{(l)}(N)\right]^T,$$
$$l = 0,1,2,\ldots,L-1, \qquad (14)$$

where

$$\mathbf{E}_l = \mathbf{diag}\left[1 \ldots e^{j(i-1)\omega_{Dl}t_s} \ldots e^{j(N-1)\omega_{Dl}t_s}\right].$$

In several publications, sample weighting is used only for the selection of minimized and non-minimized samples (e.g., WeCAN and related algorithms), with no chance of selecting any specific combinations of signals, filters, and Doppler frequencies [3], [5], [11], [13]. This is relevant because the introduction of fully optional weights significantly complicates computation. In contrast, we use different weights for all individual side lobes and crosstalk as a benefit.

Modifications of the above-derived metric expressions, including weights and Doppler effect, are shown separately for the ISL and PSL metrics.

1) MINIMUM ISL CRITERION

By introducing weights into the ISL metric, Eq. (6) can be converted into the following form:

$$\text{ISL} = \sum_{n=1-N,n\neq0}^{N-1}\left[\sum_{m=1}^{M} |w_{mm}(n)z_{mm}(n)|^2\right]$$
$$+ \sum_{n=-N+1}^{N-1}\sum_{\mu=1}^{M}\sum_{m=1,m\neq\mu}^{M} |w_{m\mu}(n)z_{m\mu}(n)|^2. \qquad (15)$$

The inclusion of signals with selected Doppler frequency shifts ω_{Dl}, requires further addition of the respective filter outputs to ISL metric (15). Written in a more effective form, it finally yields

$$\text{ISLD} = \sum_{l=0}^{L-1}\sum_{n=-N+1}^{N-1}\sum_{\mu=1}^{M}\sum_{m=1}^{M}\left[\left|w_{m\mu}^{(l)}(n)z_{m\mu}^{(l)}(n)\right|^2\right.$$
$$\left. - \delta(n)\left[w_{mm}^{(l)}(0)\right]^2\delta_{m\mu}C^2\right], \qquad (16)$$
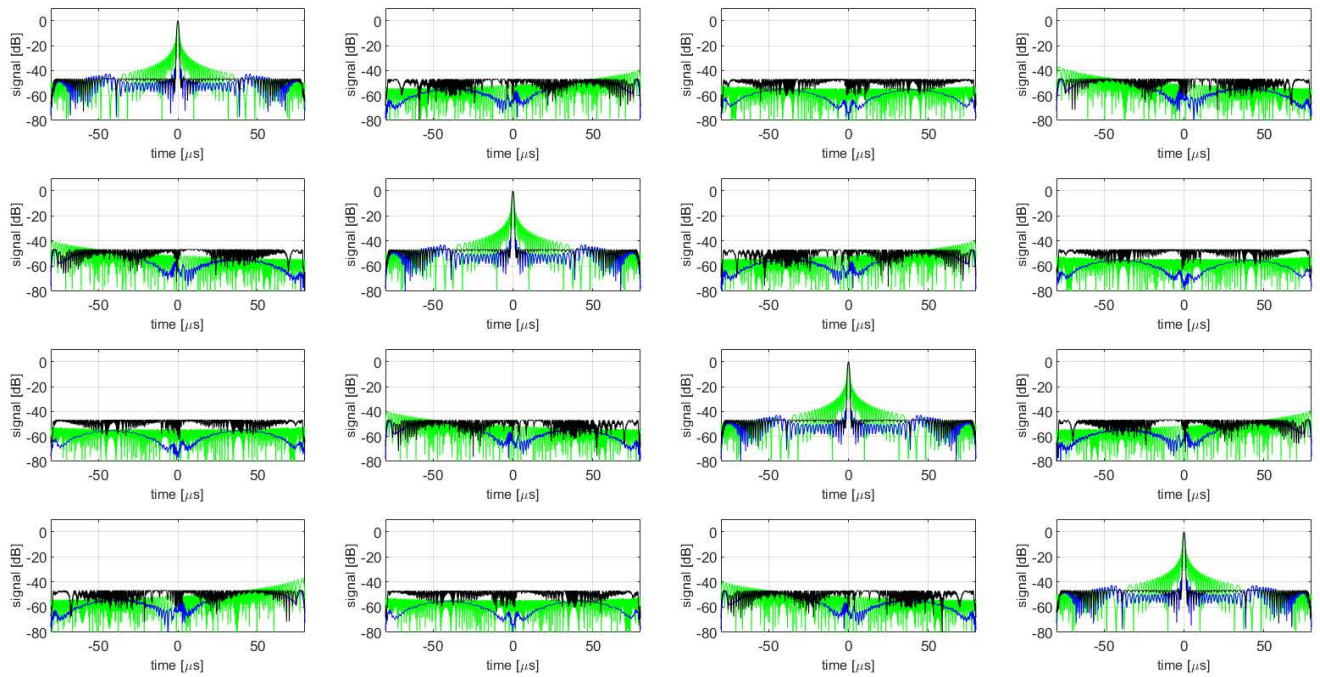
FIGURE 1. Responses of matched filter (green) and mismatched filters optimized by the both ISL (blue) and PSL (black) criteria for FD LFM signals, M = 4 and N = 500.

where $z_{m\mu}^{(l)}(n)$ is the nth sample of the convolution, $\mathbf{z}_{m\mu}^{(l)} = \mathbf{x}_m^{(l)} * \mathbf{q}_\mu$, and $w_{m\mu}(n) \in \langle 0, 1 \rangle$ are the weights of the individual side lobes and crosstalk, respectively.

The ISL metric is only a specific case of the ISLD metric at $L = 1$. Therefore, we no longer consider the ISL metric separately.

For further description, the matrix form of Eq. (16) is more advantageous. To do this, we express the convolution $\mathbf{z}_{m\mu}^{(l)}$ using the Toeplitz matrices $\boldsymbol{\Lambda}_m^{(\mathbf{l})}$ for each frequency $\omega_{\mathrm{D}l}$ and introduce the weight matrices

$$\mathbf{W}_{m\mu}^{(\mathbf{l})} = \mathbf{diag}\left[w_{m\mu}^{(l)}(-N), \ldots, w_{m\mu}^{(l)}(N) \right] \quad (17)$$

$$\mathbf{z}_{m\mu}^{(l)} = \mathbf{x}_m^{(l)} * \mathbf{q}_\mu = \boldsymbol{\Lambda}_m^{(\mathbf{l})} \mathbf{q}_\mu, \quad (18)$$

where

$$\boldsymbol{\Lambda}_m^{(\mathbf{l})} = \begin{bmatrix} x_m^{(l)}(1) & 0 & 0 & 0 \\ x_m^{(l)}(2) & x_m^{(l)}(1) & 0 & 0 \\ x_m^{(l)}(3) & x_m^{(l)}(2) & \ddots & 0 \\ \vdots & \vdots & \ddots & 0 \\ x_m^{(l)}(N) & x_m^{(l)}(N-1) & \cdots & x_m^{(l)}(1) \\ 0 & x_m^{(l)}(N) & \cdots & x_m^{(l)}(2) \\ \vdots & 0 & 0 & \vdots \\ 0 & \cdots & \cdots & x_m^{(l)}(N) \end{bmatrix}.$$

Now we introduce matrices $\check{\boldsymbol{\Lambda}}_m$ composed of products $\mathbf{W}_{m\mu}^{(l)} \cdot \boldsymbol{\Lambda}_m^{(l)}$ and vectors $\tilde{j}_\mu$.

$$\check{\boldsymbol{\Lambda}}_{\boldsymbol{\mu}} = \begin{bmatrix} \mathbf{W}_{1\mu}^{(0)} \boldsymbol{\Lambda}_1^{(0)} \\ \mathbf{W}_{2\mu}^{(0)} \boldsymbol{\Lambda}_2^{(0)} \\ \vdots \\ \mathbf{W}_{M\mu}^{(0)} \boldsymbol{\Lambda}_M^{(0)} \\ \mathbf{W}_{1\mu}^{(1)} \boldsymbol{\Lambda}_1^{(1)} \\ \vdots \\ \mathbf{W}_{M\mu}^{(1)} \boldsymbol{\Lambda}_M^{(1)} \\ \vdots \\ \mathbf{W}_{M\mu}^{(L)} \boldsymbol{\Lambda}_M^{(L)} \end{bmatrix}, \quad \check{\mathbf{j}}_{\boldsymbol{\mu}} = \begin{bmatrix} \mathbf{j}_{1\mu}^{(0)} \\ \mathbf{j}_{2\mu}^{(0)} \\ \vdots \\ \mathbf{j}_{M\mu}^{(0)} \\ \mathbf{j}_{1\mu}^{(1)} \\ \vdots \\ \mathbf{j}_{M\mu}^{(1)} \\ \vdots \\ \mathbf{j}_{M\mu}^{(L)} \end{bmatrix},$$

$$j_{m\mu}^{(l)}(n) = \delta_{\mu m} \cdot \delta_{0n}. \quad (19)$$

It is easy to determine that relation (9) for ISL is replaced by (20) for the new metric ISLD, incorporating sample weights and Doppler-affected signals:

$$\mathrm{ISLD} = \sum_{\mu=1}^{M} \left\| \check{\boldsymbol{\Lambda}}_{\boldsymbol{\mu}} \cdot \mathbf{q}_\mu - C \check{\mathbf{J}}_\mu \right\|^2. \quad (20)$$

The choice of weight vector elements $\mathbf{w}_{m\mu}^{(l)}$ allows us to adapt the optimization to a wide range of conditions. For example, when $w_{m\mu}^{(l)}(n) = 1$, all side lobes and crosstalk are minimized except for the central samples of the output signals for $n = 0$ at

$m = \mu$, which are bound by the normalization conditions $\mathbf{x}_m^T \cdot \mathbf{q}_m \equiv z_{mm}(0) = C$. If we choose $C = N$, matched filters, and constant signal modules, then this criterion becomes identical to the criteria used in [1]–[3] when optimizing signals using the CAN methods.

However, this more general introduction of weights allows us to significantly increase the side lobes and crosstalk suppression, or to simplify calculations at the cost of only minimal deterioration of the other parameters.

In addition, it was found that the crosstalk ($m \neq \mu$) deterioration caused by the Doppler effect was insignificant. Thus, the complexity of the calculations can be significantly reduced by excluding these samples from the minimization by choosing $\mathbf{w}_{m\mu}^{(l)} = \mathbf{0}$ for $m \neq \mu$ and $l > 0$.

2) MINIMUM PSL CRITERION

The inclusion of the signals affected by the Doppler shift in PSL optimization can be performed in a manner similar to the ISL criterion. By including weights in this expression and considering the normalization conditions $\mathbf{x}_m^T \cdot \mathbf{q}_m \equiv z_{mm}^{(0)}(0) = C$, the PSL metric is transformed into the following form:

$$
\begin{aligned}
\mathrm{PSLD} &= \left\| \check{\mathbf{\Lambda}}_{\boldsymbol{\mu}} \cdot \mathbf{q}_{\mu} - C \check{\mathbf{J}}_{\mu} \right\|_{\infty} \\
&= \max_{\mu} \left\| \check{\mathbf{\Lambda}}_{\boldsymbol{\mu}} \cdot \mathbf{q}_{\mu} - C \check{\mathbf{J}}_{\mu} \right\|_{\infty}.
\end{aligned}
\tag{21}
$$

In case, if we apply optimization only to the filter coefficients, we can minimize metric (21) separately for each filter, as in the case of minimum ISL criterion

$$
\mathbf{q}_{\mu} = \arg \left\{ \min_{\mathbf{q}_{\mu}} \left\| \check{\mathbf{\Lambda}}_{\boldsymbol{\mu}} \cdot \mathbf{q}_{\mu} - C \check{\mathbf{J}}_{\mu} \right\|_{\infty} \right\}.
\tag{22}
$$

This task can be solved using the QCQP methods, [26], [27].

When optimizing the filters, weights of the samples near the maximum of the main lobe were used. For frequency-diversified (FD) signals, the total bandwidth BW of the entire set of signals $\{\mathbf{x}_m\}_{m=1}^{M}$ is larger than the bandwidth B of a single signal.

$$
BW = [(M-1)\kappa + 1]B, \quad \kappa > 1.
\tag{23}
$$

The sampling period T_s is determined by the bandwidth BW of the entire signal set, $T_s \leq 1/BW$, whereas the width of the main lobe T_c corresponds to the bandwidth of one signal $T_c \approx 2/B$. Therefore, when optimizing the parameters, it is desirable to omit at least as many samples P (around the maximum of the main lobe) as corresponds to the bandwidth of signal B.

$$
P \geq \frac{T_c}{T_s} - 1 = 2\frac{BW}{B}.
\tag{24}
$$

For example, in the examples presented in this paper, we used $M = 4$, $\kappa = 1.3$, and $P \geq 9$. The lower limit of P corresponds to the bandwidth of the single signal. Skipping a larger number of samples partially deteriorated the detection of weaker targets. In our experience with optimization, dropping up to 15 samples does not essentially degrade this parameter

but rather significantly improves the side lobes and crosstalk suppression. Fig. 2 shows the dependence of SNR loss on the number of omitted samples. We see that the SNR loss is optimal at P from 8 to 11 samples for all displayed methods except of that of using minISL and NLFM initial modulation. The latter exhibits a broad minimum at P around 15. Furthermore, it can be stated that the SNR loss minima are very low except of that achieved by the minimum PSL method with LFM modulation.
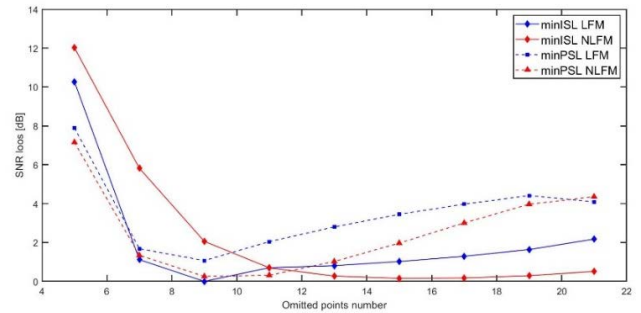

FIGURE 2. Dependence of the SNR loss of the mismatched filters on the number of omitted samples around the main lobe peak.

In Fig. 3, we can observe the effect of the Doppler shift on side-lobe suppression. We see that if the Doppler effect is not assumed in the optimization, the side-lobe level deteriorates by $5 - 10$ dB compared to the filters optimized for the Doppler shift.

III. SWAP ALGORITHM
A. ALGORITHM DESCRIPTION

To minimize both metrics, even for signal optimization, we modify the relations for the ISL and PSL metrics using the fact that the convolution is a commutative operation.

Then we can write the elements $\mathbf{z}_{m\mu}$ of the matrix $\mathbf{Z}$ in two ways

$$
\mathbf{z}_{m\mu} = \mathbf{x}_m * \mathbf{q}_{\mu} = \mathbf{q}_{\mu} * \mathbf{x}_m.
\tag{25}
$$

This formal arrangement leads to an analogous extension of the convolution expressed in (4) using the new Toeplitz matrix $\mathbf{\Pi}$ compiled from the vectors of filter coefficients $\mathbf{q}_{\mu}$, similar to the arrangement of the matrix $\mathbf{\Lambda}$ created from the vectors $\mathbf{x}_m$

$$
\begin{aligned}
\mathbf{Z} &\equiv \begin{bmatrix} \mathbf{z}_{11} & \cdots & \mathbf{z}_{M1} \\ \vdots & & \vdots \\ \mathbf{z}_{1M} & \cdots & \mathbf{z}_{MM} \end{bmatrix} \\
&= \mathbf{\Lambda}.\mathbf{Q} = \mathbf{\Lambda}. \begin{bmatrix} q_1(1) & \cdots & q_M(1) \\ \vdots & & \vdots \\ q_1(N) & \cdots & q_M(N) \end{bmatrix},
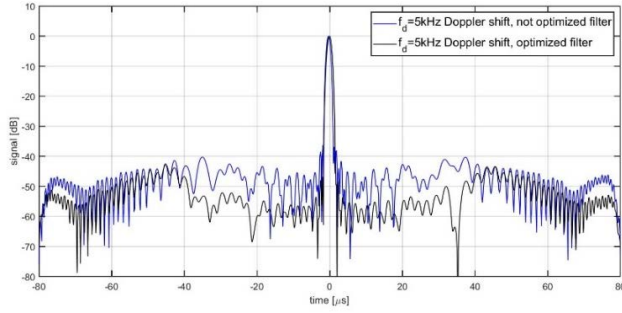\end{aligned}
\tag{26}
$$

FIGURE 3. Comparison of outputs of mismatched filters, optimized by the minimum ISL criteria including Doppler effect (black line) and without the Doppler effect (blue line). FD LFM signals with the Doppler shift of 5 kHz.

$$
\mathbf{S} \equiv \begin{bmatrix} \mathbf{z}_{11} & \cdots & \mathbf{z}_{1M} \\ \vdots & & \vdots \\ \mathbf{z}_{M1} & \cdots & \mathbf{z}_{MM} \end{bmatrix}
$$

$$
= \mathbf{\Pi}.\mathbf{X} = \mathbf{\Pi}. \begin{bmatrix} x_1(1) & \cdots & x_M(1) \\ \vdots & & \vdots \\ \vdots & & \vdots \\ x_1(N) & \cdots & x_M(N) \end{bmatrix}, \quad (27)
$$

where

$$
\mathbf{\Pi} = \begin{bmatrix} \mathbf{\Pi}_1 \\ \mathbf{\Pi}_2 \\ \vdots \\ \vdots \\ \mathbf{\Pi}_M \end{bmatrix};
$$

$$
\mathbf{\Pi}_\mu = \begin{bmatrix} q_\mu(1) & 0 & \ldots & 0 \\ q_\mu(2) & q_\mu(1) & \ddots & \vdots \\ \vdots & q_\mu(2) & \ddots & 0 \\ q_\mu(N) & \vdots & \ddots & q_\mu(1) \\ 0 & q_\mu(N) & \ddots & q_\mu(2) \\ \vdots & \ddots & \ddots & \vdots \\ 0 & \ldots & 0 & q_\mu(N) \end{bmatrix}.
$$

It is obvious that both metrics (7) and (12) can also be written symmetrically using matrix $\mathbf{\Pi}$ as follows:

$$
\text{ISL} = \| \mathbf{\Lambda}.\mathbf{Q} - C\mathbf{J} \|^2 = \| \mathbf{\Pi}.\mathbf{X} - C\mathbf{J} \|^2, \quad (28)
$$

$$
\text{PSL} = \| \mathbf{\Lambda}.\mathbf{Q} - C\mathbf{J} \|_\infty = \| \mathbf{\Pi}.\mathbf{X} - C\mathbf{J} \|_\infty. \quad (29)
$$

In case we want to include the Doppler shift effect in both metrics, we must modify the matrices $\mathbf{\Pi}_\mu$ in (27) into the form of $\mathbf{\Pi}_\mu^{(l)} = \mathbf{\Pi}_\mu \cdot \mathbf{E}_l$. Then, by including the sample weights $w_{m\mu}^{(l)}(n)$ we can create the following

matrices and vectors:

$$
\mathbf{\breve{\Pi}}_m = \begin{bmatrix} \mathbf{W}_{m1}^{(0)}\mathbf{\Pi}_1^{(0)} \\ \mathbf{W}_{m2}^{(0)}\mathbf{\Pi}_2^{(0)} \\ \vdots \\ \mathbf{W}_{mM}^{(0)}\mathbf{\Pi}_M^{(0)} \\ \mathbf{W}_{m1}^{(1)}\mathbf{\Pi}_1^{(1)} \\ \vdots \\ \mathbf{W}_{mM}^{(1)}\mathbf{\Pi}_M^{(1)} \\ \vdots \\ \mathbf{W}_{mM}^{(L)}\mathbf{\Pi}_M^{(L)} \end{bmatrix}, \quad \mathbf{\breve{j}}_m = \begin{bmatrix} \mathbf{j}_{1m}^{(0)} \\ \mathbf{j}_{2m}^{(0)} \\ \vdots \\ \mathbf{j}_{Mm}^{(0)} \\ \mathbf{j}_{1m}^{(1)} \\ \vdots \\ \mathbf{j}_{Mm}^{(1)} \\ \vdots \\ \mathbf{j}_{Mm}^{(L)} \end{bmatrix};
$$

$$
j_{m\mu}^{(l)}(n) = \delta_{\mu m}.\delta_{0n}. \quad (30)
$$

Metrics (28) and (29) could then be transformed in

$$
\text{ISLD} = \sum_{\mu=1}^M \left\| \mathbf{\breve{\Lambda}}_\mu \cdot \mathbf{q}_\mu - C\mathbf{\tilde{J}}_\mu \right\|^2
$$

$$
= \sum_{m=1}^M \left\| \mathbf{\breve{\Pi}}_m \cdot \mathbf{x}_m - C\mathbf{\breve{J}}_m \right\|^2 \quad (31)
$$

$$
\text{PSLD} = \max_\mu \left\| \mathbf{\breve{\Lambda}}_\mu \cdot \mathbf{q}_\mu - C\mathbf{\breve{J}}_\mu \right\|_\infty
$$

$$
= \max_m \left\| \mathbf{\breve{\Pi}}_m \cdot \mathbf{x}_m - C\mathbf{\breve{J}}_m \right\|_\infty \quad (32)
$$

This seemingly formal arrangement allows the achievement of a further significant improvement in the side-lobe suppression by an iterative procedure. This is because the strict requirement for a complex envelope amplitude was waived. Owing to the good linearity of current high-power amplifiers, the requirement for PAR can be slightly relaxed, as mentioned in the introduction. Then, the optimization of the metrics expressed by matrices $\mathbf{\breve{\Pi}}_m$ (29) and (30) can be used to calculate new signal vectors from the already determined filter coefficients.

For the minimum ISL criterion, we first obtain the filter coefficients $\mathbf{q}_\mu$ by minimizing (31), as follows:

$$
\mathbf{q}_\mu = \arg \left\{ \min_{\mathbf{q}_\mu} \left\| \mathbf{\breve{\Lambda}}_\mu \cdot \mathbf{q}_\mu - C\mathbf{\tilde{J}}_\mu \right\|^2 \right\} \quad (33)
$$

In the next step, we used the second expression (31) to obtain the new signal vectors:

$$
\mathbf{x}_m = \arg \left\{ \min_{\mathbf{x}_m} \left\| \mathbf{\breve{\Pi}}_m \cdot \mathbf{x}_m - C\mathbf{\breve{J}}_m \right\|^2 \right\} \quad (34)
$$

The entire procedure can be repeated until the side-lobe suppression reaches the required level and the SNR loss and PAR values are within an acceptable interval.

The same procedure can be performed for the minimum PSL criterion. We calculated the optimized filters for the selected signals $\mathbf{x}_m$:

$$
\mathbf{q}_\mu = \arg \left\{ \min_{\mathbf{q}_\mu} \left\| \mathbf{\breve{\Lambda}}_\mu \cdot \mathbf{q}_\mu - C\mathbf{\breve{J}}_\mu \right\|_\infty \right\}, \quad (35)
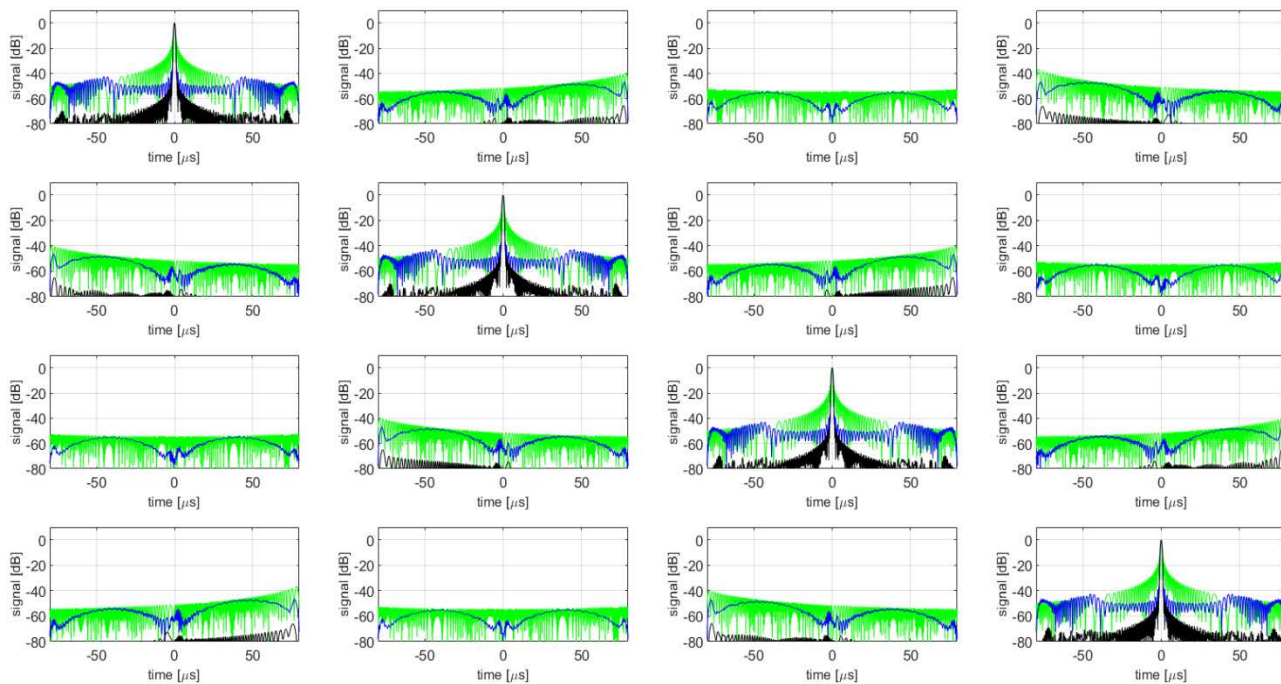$$

FIGURE 4. Side lobes and crosstalk suppression using SWAP algorithm for signal and filter optimization in the case of four FD LFM signals (in columns). Each row stands for one filter. The ISL optimization criterion is used. The green line represents the matched filter, the blue line represents the mismatched filter, the black line represents the mismatched filter after 60 exchanges.

TABLE 1. The SWAP algorithm.

Step 0: Create a FD-LFM or FD-NLFM signal set
Step 1: Build a matrix $\breve{\boldsymbol{\Lambda}}_\mu$ from vectors $^i\mathbf{x}_m$
Step 2: Calculate filters $^i\mathbf{q}_m$
Step 3: Build the matrix $\bar{\boldsymbol{\Pi}}_m$ from the filters $^i\mathbf{q}_\mu$
Step 4: Calculate the new signal $^{i+1}\mathbf{x}_m$
Step 5: Repeat steps 1 to 4 until the selected criterion is achieved.

and then the optimized signals for these filters

$$\mathbf{x}_m = \arg\left\{ \min_{\mathbf{x}_m} \left\| \breve{\boldsymbol{\Pi}}_m \cdot \mathbf{x}_m - C\breve{\mathbf{J}}_m \right\|_\infty \right\}. \tag{36}$$

The described procedure, which we call the SWAP algorithm, can be generalized into the steps listed in Table 1. However, it should be noted that the SWAP algorithm does not retain a constant signal envelope.

Fig. 4 and 5 present illustrations of the side lobes and crosstalk suppression using the SWAP algorithm.

In Fig. 4, the results of the four FD LFM signals (in columns) when the minimum ISL criterion is used are shown. In this diagram, each row includes the output from the same filter. We can see that the side lobes and crosstalk are suppressed even more (by 20 dB) compared to the matched filter using 60 exchanges (swaps).

A comparison of the ISL and PSL criteria is shown in Fig. 5. We can see that while at the start of the procedure

(mismatched filters), the results of both criteria are quite comparable; after 40 swaps, the side-lobe suppression achieved by the ISL criterion is up to 15 dB better.
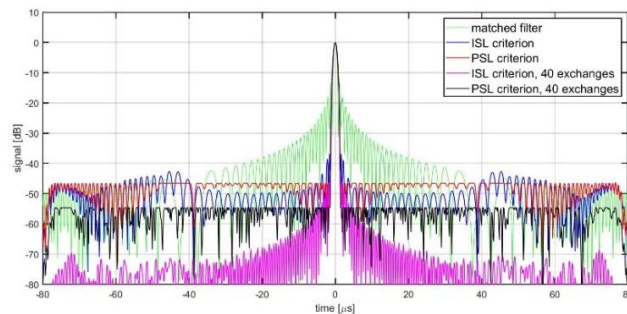

FIGURE 5. Comparison of side lobe suppression by the SWAP algorithm using ISL and PSL criteria. Initial signal FD LFM is used.

Similar dependencies were obtained when the Doppler effect was included in the optimization. An example of successful side-lobe suppression with the ISL criterion, even when the signal is modulated by a 5 kHz Doppler shift, is shown in Fig. 6. The side lobes fall below -70 dB after 20 exchanges.

B. ALGORITHM EXAMINATION

To facilitate further illustration, we introduce a new characteristic SL representing the mean sidelobes and crosstalk level. This is the power ratio of the mean absolute value of the side lobes and the crosstalk to the main lobe
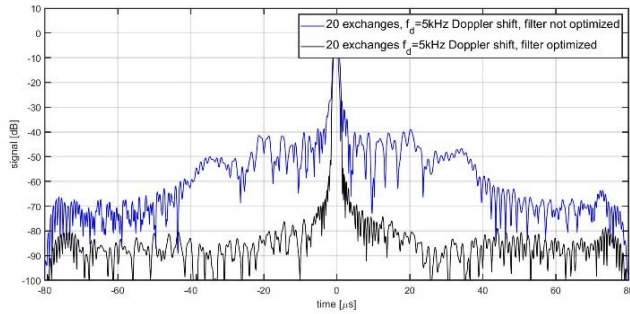
FIGURE 6. Comparison of the filter responses to signals, modulated by a Doppler shift of 5 kHz after 20 swaps. The blue line - neither filters nor signals are optimized for the Doppler shift, the black line - optimization for the Doppler shift. The minimum ISL criterion is used.

maximum, $z_{m,m}^{(0)}(0) = C$.

$$
\text{SL} = 20.\log \left[\frac{1}{M^2 (2N - 1 - P) C} \right.
$$
$$
\left. \times \sum_{m,\mu,n} \left[\left| w_{m,\mu}^{(0)}(n) . z_{m,\mu}^{(0)}(n) \right| - C\delta_{m,\mu}\delta(n) \right] \right]. \quad (37)
$$

As a measure of algorithm convergence, we consider the norm of the difference between the subsequent approximations of signal samples or filter coefficient matrices, $\left\| {}^{i+1}\mathbf{X} - {}^{i}\mathbf{X} \right\|$, or $\left\| {}^{i+1}\mathbf{Q} - {}^{i}\mathbf{Q} \right\|$.
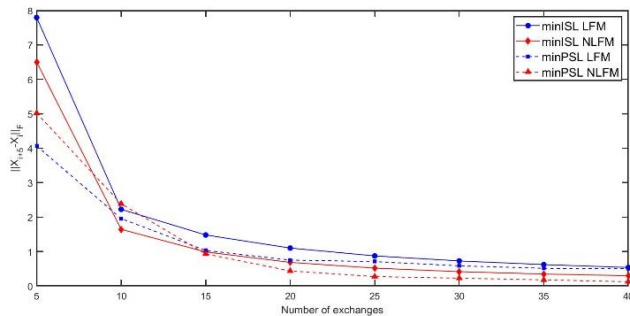

FIGURE 7. Dependence of the signal difference norm $\left\| {}^{i+1}\mathbf{X} - {}^{i}\mathbf{X} \right\|$ during SWAP optimization.

An example displayed in Fig. 7 shows that a substantial approximation occurs during the first ten or 20 exchanges. It is worth to note that matrix $\left\| {}^{i+1}\mathbf{X} - {}^{i}\mathbf{X} \right\|$ consists of $N \times M = 2\,000$ elements, therefore the average difference between the signal samples of the subsequent iterations is less than 5×10^{-4} after only 15 exchanges (swaps).

From Fig. 8 – 10, it is evident that during the SWAP algorithm, the side lobes and crosstalk are continually reduced, but simultaneously, the SNR loss and PAR increase slightly. All of these parameters changed until the 10th exchange mainly.

From Fig. 8, it is clear that while the effect of the initial signal choice (i.e., LFM or NLFM) on the side lobes and crosstalk suppression is negligible, the impact of the optimization criterion selection is significant. We can also see that by using the ISL metric, the achieved SL value is improved by approximately 15 dB.
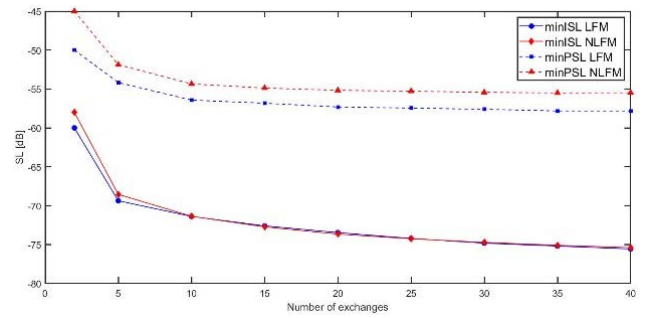

FIGURE 8. Development of the side lobe suppression depending on the number of exchanges using both minimum ISL and minimum PSL criteria.
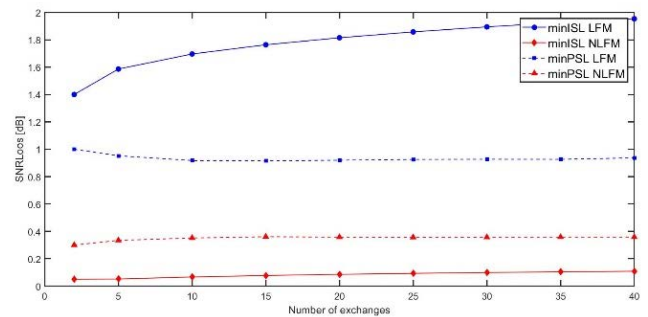

FIGURE 9. SNR loss dependence on the number of exchanges during the SWAP algorithm optimization.

In contrast, the changes in SNR loss during the SWAP algorithm, as shown in Fig. 9, are not significant and remain at acceptable levels, which is vitally important. Except for the combination of the minimum ISL criterion and FD LFM signals, the SNR loss was maintained below 1 dB.
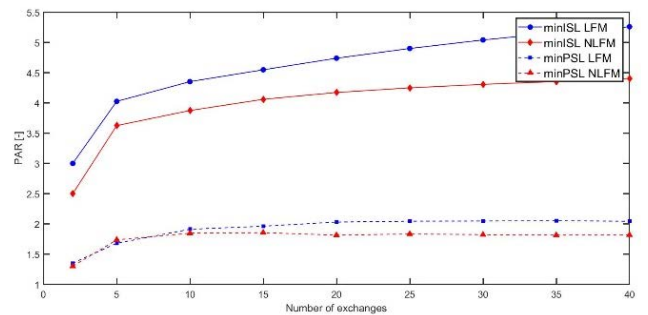

FIGURE 10. Dependence of the peak to average power ratio (PAR) on the number of swaps in the course of optimization using the SWAP algorithm.

Fig. 10 shows the dependence of PAR on the optimization criterion and initial signal modulation during the SWAP algorithm. The PAR mainly depends on the selected optimization criterion. Using the ISL metric, the PAR quantity reaches values of up to four or five after only ten swaps, which is unacceptable.

In contrast, when using the minimum PSL criterion, PAR remains under a magnitude of 2, even in the case of a higher number of swaps.

For instance, using this criterion and the NLFM initial signal, we obtain a PAR value of approximately 1.7 at 10 swaps, which is a tolerable value in modern radars.

IV. CONCLUSION

In this study, we introduce a method for the simultaneous optimization of filters and signals suitable for long-range radars with a pulse length shorter than the return time of the reflected signals. For this optimization method of cyclic approximation, we used the term SWAP. It turns out that with a partial relaxation of the requirements of constant signal amplitude and SNR loss, a significant improvement in the side lobe and crosstalk suppression can be achieved. The SWAP method also includes the optimization of signals with a Doppler shift. An important tool for achieving these results is the independent weighting of the side lobes and crosstalk for all signal and filter combinations. The properties of the SWAP algorithm are documented for specific cases using signals with the time bandwidth product $B\tau = 100$, number of signals $M = 4$, and number of signal samples $N = 500$. This method can find applications, especially for narrowband long-range radars such as 3D ground surveillance radars or weather radars.

REFERENCES

[1] P. Stoica, J. Li, and Y. Xie, "On probing signal design for MIMO radar," *IEEE Trans. Signal Process.*, vol. 55, no. 8, pp. 4151–4161, Aug. 2007.

[2] Y. Yang and R. S. Blum, "MIMO radar waveform design based on mutual information and minimum mean-square error estimation," *IEEE Trans. Aerosp. Electron. Syst.*, vol. 43, no. 1, pp. 330–343, Jan. 2007.

[3] J. Li, P. Stoica, and X. Zheng, "Signal synthesis and receiver design for MIMO radar imaging," *IEEE Trans. Signal Process.*, vol. 56, no. 8, pp. 3959–3968, Aug. 2008.

[4] T. Bai, N. Zheng, and S. Chen, "OFDM MIMO radar waveform design for targets identification," *ETRI J.*, vol. 40, no. 5, pp. 592–603, Oct. 2018. [Online]. Available: https://wileyonlinelibrary.com/journal/etri.

[5] H. He, P. Stoica, and J. Li, "Designing unimodular sequence sets with good correlations—Including an application to MIMO radar," *IEEE Trans. Signal Process.*, vol. 57, no. 11, pp. 4391–4405, Nov. 2009.

[6] A. Sajid and M. S. Alouini, "MIMO-radar waveform covariance matrix for high SINR and low side-lobe levels," *IEEE Trans. Signal Process.*, vol. 62, no. 8, pp. 2056–2065, Apr. 2014.

[7] Z. Zhou, S. Zhao, Q. Shi, and R. Zhang, "Sequence set design with min-max criterion using majorization-minimization," in *Proc. IEEE/CIC Int. Conf. Commun. China (ICCC)*, Changchun, China, Aug. 2019, pp. 550–555.

[8] J. Song, P. Babu, and D. P. Palomar, "Sequence set design with good correlation properties via majorization-minimization," *IEEE Trans. Signal Process.*, vol. 64, no. 11, pp. 2866–2879, Jun. 2016.

[9] J. Zhang, N. Xu, H. Song, and C. Zhang, "Sequence set design for waveform-agile coherent radar systems," *EURASIP J. Adv. Signal Process.*, vol. 2020, p. 31, Jul. 2020, doi: 10.1186/s13634-020-00689-0.

[10] A. Bose, I. Arriaga-Trejo, A. G. Orozco-Lugo, and M. Soltanalian, "Generaized cycling algorithms for designing unimodular sequence sets with good (complementary) correlation properties," in *Proc. IEEE 10th Sensor Array Multichannel Signal Process. Workshop (SAM)*, Jul. 2018, pp. 287–291.

[11] G. Cui, H. Li, and M. Rangaswamy, "MIMO radar waveform design with constant modulus and similarity constraints," *IEEE Trans. Signal Process.*, vol. 62, no. 2, pp. 343–353, Jan. 2014.

[12] X. Z. Dai, J. Xu, and C. M. Ye, "Low-sidelobe HRR profiling based on the FDLFM-MIMO radar," in *Proc. 1st Asian Pacific Conf. Synth. Aperture Radar*, Huangshan, China, Nov. 2007, pp. 132–135.

[13] F. Wang, C. Pang, Y. Li, and X. Wang, "Designing constant modulus sequences with good correlation and Doppler properties for simultaneous polarimetric radar," *Electronics*, vol. 7, no. 8, p. 153, Aug. 2018, doi: 10.3390/electronics7080153.

[14] L. Xu, H. Liu, S. Zhou, H. Ma, J. Zheng, and J. Wang, "Joint optimization of transmit waveform and mismatched filter with expanded mainlobe for delay-Doppler sidelobes suppression," in *Proc. Int. Conf. Radar (RADAR)*, Brisbane, QLD, Australia, Aug. 2018, pp. 19–24.

[15] P. Bezoušek and S. Karamazov, "MIMO radar signals with better correlation characteristics," *J. Electr. Eng.*, vol. 71, no. 3, pp. 210–216, Jun. 2020.

[16] W. A. Blake, "Multi-dimensional mismatch filter design optimization for radar waveforms," presented at the Int. Radar Conf., New York, NY, USA, 2016.

[17] P. Bezousek, S. Karamazov, and J. Rolecek, "Adaptive pulse compression filter in radar receiver application," in *Proc. Conf. Microw. Techn. (COMITE)*, Pardubice, Czech Republic, Apr. 2019, pp. 1–4.

[18] J. Cillier and J. Smit, "On the trade-off between mainlobe width and peak sidelobe level of mismatched pulse compression filters for linear chirp waveforms," in *Proc. Eur. Radar Conf. (EuRAD)*, Rome, Italy, Sep./Oct. 2009, pp. 9–12.

[19] L. C. Nunes, P. M. Cabral, and J. C. Pedro, "AM/AM and AM/PM distortion generation mechanisms in Si LDMOS and GaN HEMT based RF power amplifiers," *IEEE Trans. Microw. Theory Techn.*, vol. 62, no. 4, pp. 799–809, Apr. 2014.

[20] A. Katz and R. Dorval, "Linearizing high power amplifiers (with emphasis on predistortion and GaN devices)," in *Proc. IEEE Top. Conf. Power Amplif. Wireless Radio Appl.*, Santa Clara, CA, USA, Jan. 2012, pp. 33–36.

[21] P. Hindle, "Extremely high-power GaN devices," *Microw. J.*, vol. 62, no. 9, pp. 20–32, Sep. 2019.

[22] I. Takenaka, K. Ishikura, K. Asano S. Takahashi, Y. Murase, Y. Ando, H. Takahashi, and C. Sasaoka, "High-efficiency and high-power microwave amplifier using GaN-on-Si FET with improved high-temperature operation characteristics," *IEEE Trans. Microw. Theory Techn.*, vol. 62, no. 3, pp. 502–512, Mar. 2014.

[23] M. Forouzanfar and M. Joodaki, "Systematic design of hybrid high power microwave amplification using large gate periphery GaN HEMTs," *AEU-Int. J. Electron. Commun.*, vol. 84, pp. 225–233, Feb. 2018.

[24] W. DeMore, "Gauging the state of GaN power amplification," Analog Devices, Norwood, MA, USA, Tech. Article, 2019.

[25] B. Pavel, D. Matousek, and L. Rejfek, "Nonlinear distortion in a microwave high power amplifier," in *Proc. 29th Int. Conf. Radioelektronika (RADIOELEKTRONIKA)*, Pardubice, Czech Republic, Apr. 2019, pp. 136–139.

[26] O. Rabaste and L. Savy. (2014). *Quadratically Constrained Quadrature Programs for Mismatched Filter Optimization with Radar Applications.* [Online]. Available: https://hal.archives-ouvertes.fr/hal-01080572

[27] M. Grant and S. Boyd. (Jan. 2020). *CVX: MATLAB Software for Disciplined Convex Programming, Version 2.2.* [Online]. Available: http://cvxr.com/cvx

PAVEL BEZOUŠEK was born in Ostrava, Czechoslovakia, in 1943. He received the M.S. and Ph.D. degrees from Czech Technical University in Prague, in 1966 and 1980, respectively. He worked with the Radio Research Institute of Tesla Pardubice, from 1966 to 1994, where he was engaged in microwave circuits and systems design. Since then, he has been with the University of Pardubice, where he is currently a Full Professor with the Faculty of Electrical Engineering and Informatics, studying radar systems design.

SIMEON KARAMAZOV was born in Pardubice, Czechoslovakia, in 1963. He received the Ing. degree from Czech Technical University in Prague, in 1987, and the Ph.D. degree in solid-state physics and semiconductors from the University of Pardubice, in 1994. Since 1991, he has been working with the University of Pardubice, where he is currently a Full Professor with the Department of Mathematics and Physics, Faculty of Electrical Engineering and Informatics.

● ● ●